Improvement of interlaminar mechanical properties of CARALL based on nanofiller interface reinforcement and other fabrication techniques

Huiming Ning[1], Yuan Li[2] and Ning Hu[1,*]

[1]Department of Mechanical Engineering, Chiba University, 1-33 Yayoi-cho, Inage-ku, Chiba 263-8522, Japan

[2]Department of Nanomechanics, Tohoku University, 6-6-01 Aramaki-Aza-Aoba, Aoba-ku, Sendai 980-8579, Japan

* Corresponding author: huning@faculty.chiba-u.jp

Abstract: Improvement of interlaminar mechanical properties in carbon fiber aluminum laminates (CARALL) fabricated by carbon fiber reinforced plastic (CFRP) layers combined with aluminum alloy layers was studied. Various toughing methods including acid etching treatment and patterned structure manufacturing on the surfaces of aluminum alloy layers, and addition of nanofiller, i.e., VGCF, to the interface of CFRP and aluminum alloy through powder method, were employed to improve the mechanical properties of CARALL. Experimental results of double cantilever beam (DCB) tests indicated the improvement on the interlaminar mechanical properties of Mode-I fracture from much higher critical load P_c and fracture toughness G_{IC} when using the acid etching treatment and VGCF addition. The acid etching treatment sample with VGCF 20 g/m² possesses the highest G_{IC}, which is 41 times higher than that of the sample without any treatment. The patterned structure manufacturing on the surfaces of aluminum alloy layers can further improve the fracture properties of CARALL without adding VGCF. While VGCF was included in CARALL specimens, the patterned structure manufacturing has a minor effect on the Mode-I interlaminar mechanical properties. Crack propagation and fracture surface have also been observed to interpret the improvement mechanism.

Keywords: Carbon fiber aluminum laminates (CARALL), vapor grown carbon fiber (VGCF), fracture toughness, interlaminar mechanical properties.

1. Introduction

Carbon fiber aluminum laminates (CARALL) are a kind of FML (fiber metal laminates) materials which are hybrid composite structures based on thin sheets of metal alloys and plies of fiber reinforced polymeric (FRPs) materials combining the advantages of metallic materials and fiber reinforced matrix systems. Metallic materials are for instance isotropic, have a high bearing strength and impact resistance and are easy to repair, while fiber reinforced matrix systems have excellent fatigue characteristics and high strength and stiffness. The fatigue and corrosion problems of metallic materials and the low bearing strength, impact resistance and reparability of fiber reinforced matrix systems can be overcome by the combination [1]. Nevertheless, laminates, and CARALL is no exception, have some disadvantages as well. Due to the combination of different materials, new failure mechanisms are introduced. One of such a mechanism is delamination, which can have serious consequences for the overall stiffness of the material, especially in those cases where compressive or shear loadings are dominate. The relatively weak bonding between metal/polymer interfaces still remains a problem to be solved.

In order to solve this problem, surface treatment methods (e.g. acid treatment, anodizing, and

patterned structure manufacturing etc.) were employed by many researches to improve the interface mechanical properties of FMLs [2-7]. Kim *et al.* [3] systematically investigated the influence of surface morphology on the adhesion strength of a CFRP/Steel bond by incorporating micro-periodic line patterned surface on the metal substrate. They pointed out that the major source of strength enhancement caused by metal surface topography modification in polymer/metal bonded joints is the transition from interfacial to cohesive failure. Nano- and micro-scale surface treatment effects on adhesion strength improvement for CFRP/aluminum interfaces were investigated by Jang *et al.* [6]. Micro-scale line pattern was made on the aluminum surface by using conventional photolithography and acid etching. Anodizing process was employed to create uniform nano-porous morphology across the whole line pattern region on the aluminum specimen. The results showed that the specimen with nano-scale morphology in micro-scale line pattern resulted in the highest maximum load bearing capacity compared with that of only with micro-scale line pattern.

With excellent mechanical properties, nanofillers (carbon nanotubes (CNTs), nanoclays, vapor grown carbon fiber (VGCF), etc.) are considered as ideal reinforcement candidates to the matrix or the interface of laminate composite to improve its mechanical properties. For instance, Jen *et al.* [8] observed that the incorporation of 1.0 wt.% SiO_2 nanoparticles into interfaces among CFRP plies resulted in the increase of the overall in-plane tensile strength and stiffness of CFRP, but little improvement in fatigue behavior. A prepared VGCF paste interlayer was inserted into the interface between two $[0^o]_7$ CFRP sublaminates by Arai *et al.* [9], and revealed that the Mode-I fracture toughness was enhanced by 50%. However, till now, there has been no report about using nanofillers as the reinforcement for FML. The combined effects of various toughing methods (e.g. acid etching treatment, patterned structure manufacturing, addition of nanofiller) have not been well explored.

In this study, various toughing methods including acid etching treatment and patterned structure manufacturing on the surfaces of aluminum alloy layers, and addition of nanofiller (i.e., VGCF) to the interface of CFRP and aluminum alloy through powder method, were employed to improve the interlaminar mechanical properties of CARALL. The area density of VGCF varies at 0, 10, 20, and $30g/m^2$ at the interface. The results of DCB tests demonstrate that this new hybrid CARALL with acid etching treatment and $20g/m^2$ VGCF addition possess the highest Mode-I interlaminar fracture toughness. While the patterned structure manufacturing on the surfaces of aluminum alloy layers only has an improvement effect on the Mode-I interlaminar mechanical properties when VGCF was not dispersed into the laminate interfaces. Crack propagation and fracture surface observations of specimens using optical microscopy have also been carried out to study the toughening mechanism of the hybrid CARALL.

2. Experiments

2.1 Fabrication of specimens
To systematically investigate the effects of different toughing technologies, as shown in Table 1, 9 kinds of CARALL specimens have been fabricated in an autoclave for 3h at curing temperature of 130℃. The producing process was schematically shown in Fig. 1. The CFRP prepregs (TOHO

TENAX Co., Ltd, Japan), one commercial aluminum alloy AL2017 (TOHO Hitetsu-Kinzoku Co., Ltd, Japan) and VGCF (Showa Denko K.K, Japan) were used, where the details of the physical and mechanical properties were given in Table 2, where "A" denotes the acid-treatment, and "G" denotes patterned structure manufacturing with grooves. All of the specimens except the first kind CARALL were treated by acid etching process. In the acid etching process, the aluminum alloy layers were socked in 1mol/l nitric acid for 24h to increase their surface roughness. In addition to acid etching treatment, the aluminum alloy layers of the last four kinds of specimens were also processed with small grooves which were vertical to the fiber direction of the CFRP laminates. The dimensions of the grooves were shown in Fig. 2. Moreover, in some specimens, three different contents of VGCF, as the reinforcement for interface, were dispersed at the interface of unidirectional CFRP laminates and the aluminum alloy layers during the hand lay-up process,

Table 1. Specimen list

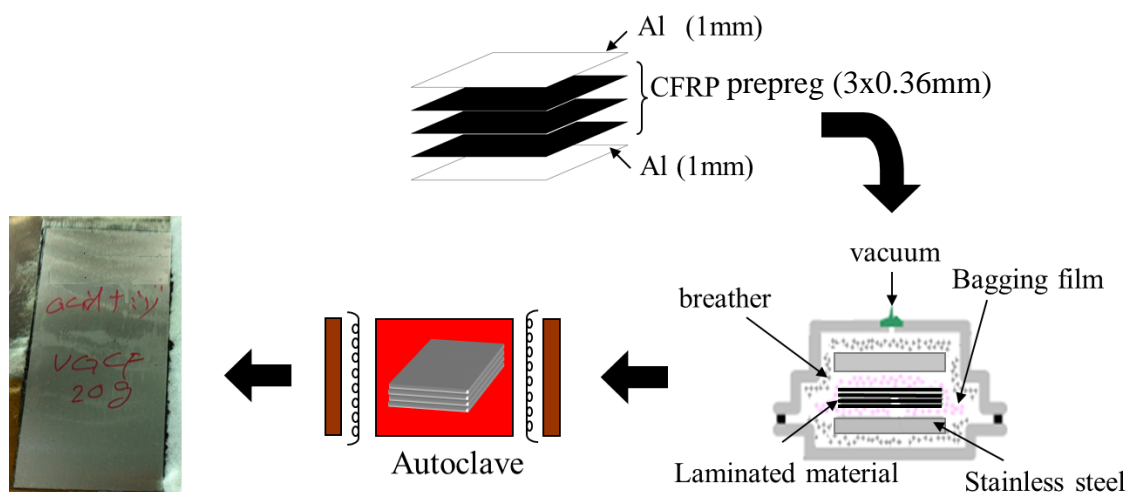| Specimens	Acid treatment	Grooved	VGCF
CARALL	—	—	—
A-CARALL	○	—	—
A-CARALL(10)	○	—	10 [g/m^2]
A-CARALL(20)	○	—	20 [g/m^2]
A-CARALL(30)	○	—	30 [g/m^2]
A-G-CARALL	○	○	—
A-G-CARALL(10)	○	○	10 [g/m^2]
A-G-CARALL(20)	○	○	20 [g/m^2]
A-G-CARALL(30)	○	○	30 [g/m^2]

Figure 1. Schematic illustration of specimen fabrication process

Table 2. Physical and mechanical properties of CFRP prepregs, AL2017 and VGCF

CFRP prepreg		VGCF	
Young's modulus (Fiber direction)	116.8GPa	Diameter	150nm
Young's modulus (Transverse direction)	8.83GPa	Length	10-20mm
CF content	63%	Aspect ratio	10-500
AL2017		Density	2.0g/cm^3
Young's modulus	80GPa	Young's modulus	273-760GPa
Tensile strength	375MPa	Tensile stress	2700-3500MPa
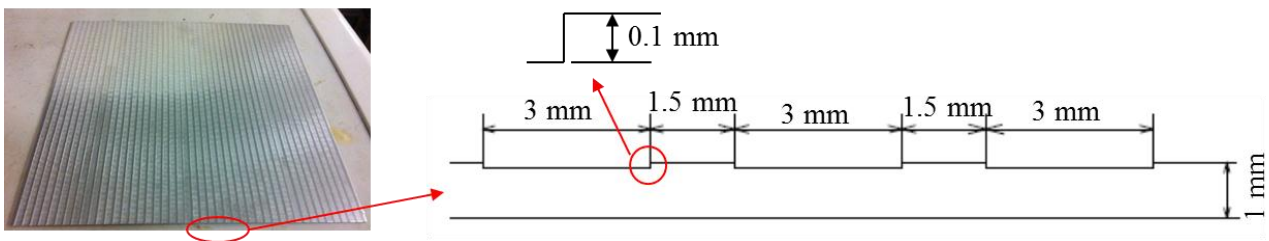
Figure 2. Dimensions of the grooves on the aluminum alloy layer

where a simple and newly-developed fabrication technology with low production cost, i.e., *powder method* [10], was employed.

2.2 DCB test procedure

In order to evaluate the Mode-I interlaminar fracture toughness, DCB tests have been carried out using a universal material testing machine at 25°C by referring to Japanese Industrial Standards (JIS) K7086 [11]. Two specimens for each type of laminate with different toughing treatments were cut from the fabricated panels, where mark lines were painted on side surface for crack length measurement. The dimensions of specimens were schematically depicted in Fig. 3.   Tensile loads
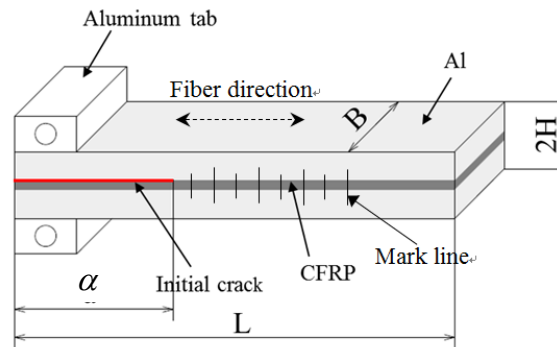
Length L=125mm; Width B=20mm; Height H=2.36mm~
Initial crack length *a*=45mm
Figure 3. Specimen for DCB tests

were applied at two aluminum tabs at one end of the specimen by using special apparatus through universal joints at a crosshead speed of 0.5mm/min. As given in Ref. [11], G_{IC} at the initial stage of crack growth and fracture resistance G_{IR} during crack propagation process can be calculated as a function of the crack growth, which is obtained by visually measuring the side surface of specimen. First, the relationship between the crack length a, and the compliance of load-COD (crack opening displacement) curve λ, are expressed in the following equation,

$$\frac{a}{2H} = \alpha_1 (B\lambda)^{\frac{1}{3}} + \alpha_0 \tag{1}$$

$$\lambda = \frac{\delta}{P} \tag{2}$$

Here δ and P stand for COD and the applied force respectively, α_0, α_1 are the fitted coefficients obtained from the experimental relation between a and λ. Then, by using the compliance method of homogeneous isotropic materials in classical fracture mechanics, G_{IC} and G_{IR} can be evaluated as follows,

$$G_{IC} = \frac{3}{2(2H)} \left(\frac{P_C}{B}\right)^2 \frac{(B\lambda_0)^{\frac{2}{3}}}{\alpha_1} \tag{3}$$

$$G_{IR} = \frac{3}{2(2H)} \left(\frac{P_R}{B}\right)^2 \frac{(B\lambda)^{\frac{2}{3}}}{\alpha_1} \tag{4}$$

where P_C is the critical load at the initialization of crack growth, and P_R the load during crack growth process, which can be obtained from load-COD curves.

3. Results and discussion

3.1 Mode-I interlaminar fracture toughness

Typical load-COD curves were plotted in Fig. 4, which shows the comparison of four representative types of specimens, i.e., CARALL, A-CARALL, A-CARALL(20), and A-G-CARALL. Critical loads at crack growth P_C for various types of specimens, which are obtained from peaks loads in Fig. 4, were shown in Fig. 5. From Figs. 4 and 5, it can be found that P_C of A-CARALL, A-CARALL(20), and A-G-CARALL were higher than that of base CARALL, which indicates the reinforcement effect of acid etching treatment, patterned surface manufacturing and VGCF interlayer. The highest P_C occurs in the case of A-CARALL(20), which is about 12 times higher than that of the base CARALL laminates and 4 times higher than that of the A-CARALL specimen.
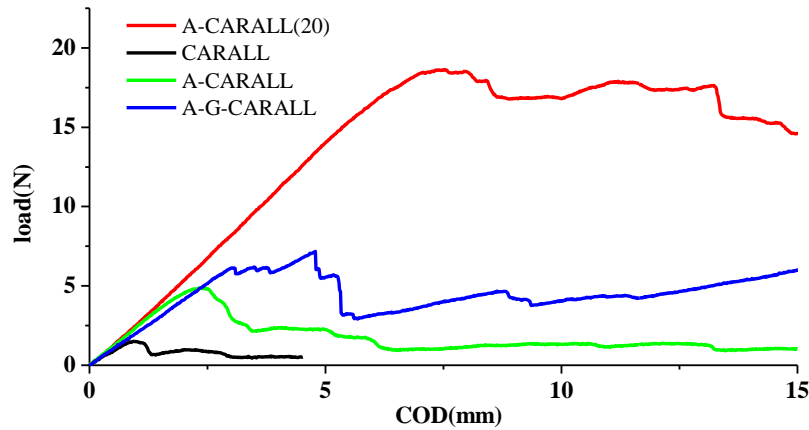
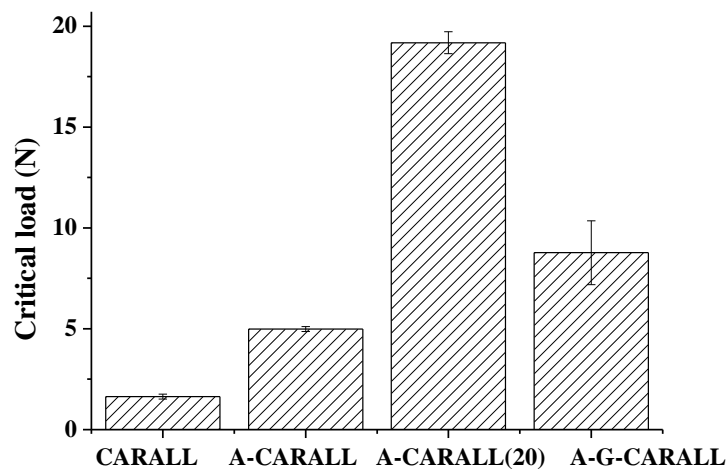Figure 4. Comparison of load-COD curves for four kinds of specimens

Figure 5. Critical load P_C for four kinds of specimens

Based on the load-COD curves of all fabricated samples and Eqs. (3-4), Mode-I fracture toughness G_{IC} and fracture resistance G_{IR} were demonstrated in Figs. 6 and 7 respectively. Note that G_{IR} was obtained by averaging the G_{IR} values of 5 points within the range of increment of crack length from 20 mm to 40 mm. For better understanding of the results from Figs. 6 and 7, two different situations were discussed. In the first situation, no VGCF was added into the specimens. In this case, it can be found from Figs. 6 and 7 that G_{IC} and G_{IR} were increased greatly for the A-CARALL and A-G-CARALL specimens. This indicates that the acid etching treatment can enhance the interlaminar mechanical properties of hybrid CARALL effectively. Without the addition of VGCF($0g/m^2$), the higher G_{IC} and G_{IR} of A-G-CARALL compared to that of A-CARALL demonstrates that the patterned surface manufacturing in the acid treatment aluminum alloy layers can further improve the interlaminar mechanical properties of hybrid CARALL. Therefore, in the case of no nanofiller, the optimal toughing technique was the combination acid treatment and patterned surface manufacturing. In the other situation, VGCF interlayer was included in the specimens. In this case, we can see from Figs. 6 and 7 that the G_{IC} of A-CARALL and A-G-CARALL specimens were both improved significantly with the addition of VGCF. In particular, the specimens with VGCF $20g/m^2$ loading have the highest fracture toughness which is of approximate 41 times higher G_{IC} than that of the pure CARALL specimen. However, as VGCF

6

content increases above $20g/m^2$, the fracture toughness tends to decrease. By increasing the VGCF content to $30g/m^2$, the G_{IC} of these specimens are approximate one half of the $20g/m^2$ specimens. Moreover, it is easy to find that although the patterned surface can improve the interlaminar mechanical properties of A-CARALL composite without VGCF addition, however, when VGCF was added into the specimens, the G_{IC} of A-G-CARALL is all lower than that of A-CARALL except A-G-CARALL(30) specimen. This indicates that the improvement effects of VGCF addition for A-W-CARALL were lower than A-CARALL specimens. Therefore, in this case, the optimal toughing method was acid treatment combined with $20g/m^2$ VGCF or $10g/m^2$ VGCF. Note that the G_{IC} of A-CARALL(20) is only slightly higher than A-CARALL(10), however, the VGCF loading is two times of A-CARALL(10). As for G_{IR}, the trend of results was almost the same as that of G_{IC}, except for the result of A-G-CARALL(20). G_{IR} of the specimens increases with the addition of VGCF, passes through a peak value (for A-CARALL at $20g/m^2$ loading, for A-G-CARALL at $10g/m^2$ loading), and then decreases.
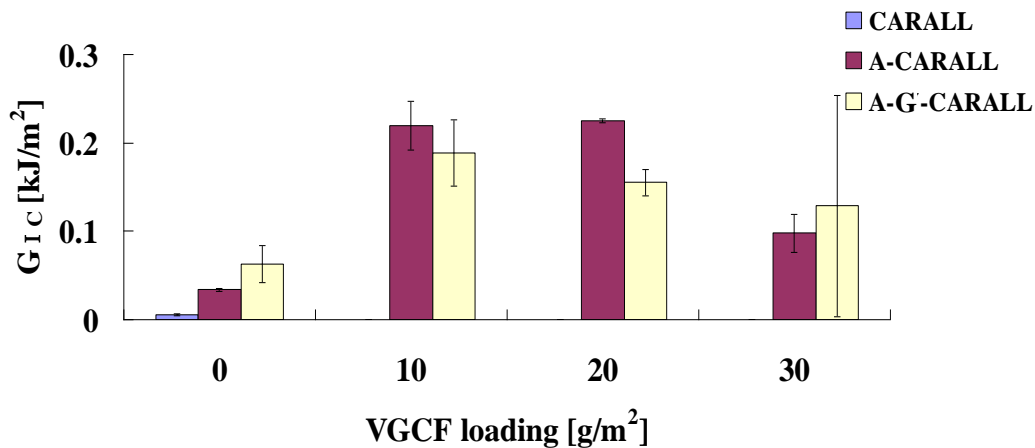
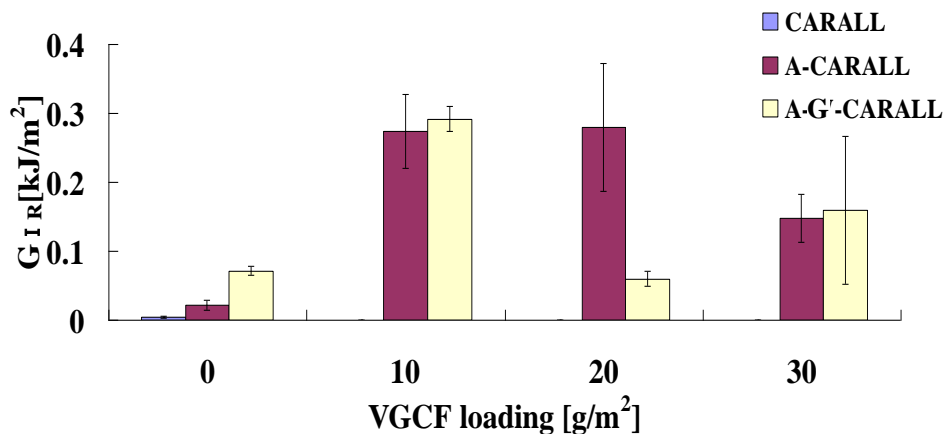Figure 6. Comparison of G_{IC} for various specimens

Figure 7. Comparison of G_{IR} for various specimens

3.2 Crack path and fracture surface observations

To uncover the relevant toughening mechanisms involved, the following experimental observations have been conducted.
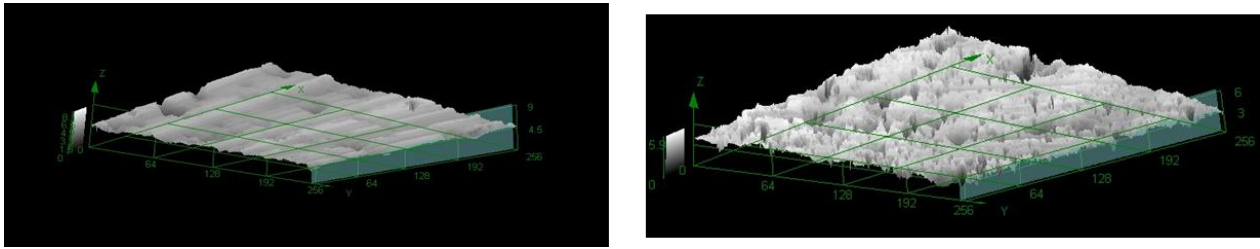
Figure 8. Surface morphology of the aluminum layers (a) before and (b) after acid etching treatment

For the first case, no VGCF was added into the specimens. Figure 8 describes the surface morphology of the aluminum layers before and after acid etching treatment respectively. It can be found that the acid etching treatment have produced a rough surface on the aluminum plate which consist of many small holes, grooves. The average diameter is about 18μm and the depth is approximately 2-5μm. When a liquid epoxy resin is applied to the rough surface, it conforms to the rough surface and tends to fill up the irregularities of the substrate surface such as microgrooves, holes. Consequently, mechanical interlock forms after the epoxy resin is cured. Due to the formed mechanical interlock, cohesive failure of the epoxy resin occurs near the interface as the epoxy is peeled away from the substrate, resulting in the crack path deviating from the interface. Such deviation of crack path away from the interface usually results in the increase of fracture surface area and requires additional energy associated with the crack propagation within the polymer. Moreover, cohesive failure, caused from the molecular decohesion of the polymer resin, expends larger energy for crack propagation than interfacial failure [4]. Furthermore, plastic energy dissipation in the bulk polymer material is effectively-induced during the crack growth in the polymer region rather than during the crack growth at the interface. Therefore, the acid etching treatment can effectively enhance the interface strength. As for the patterned structure manufacturing, the crack path deflected at the position of patterned grooves as shown in Fig. 9. Therefore, more cohesive failure occurred and more fracture surface formed during the crack propagation which explains the improvement of G_{IC} and G_{IR} compared to that of A-CARALL specimen.
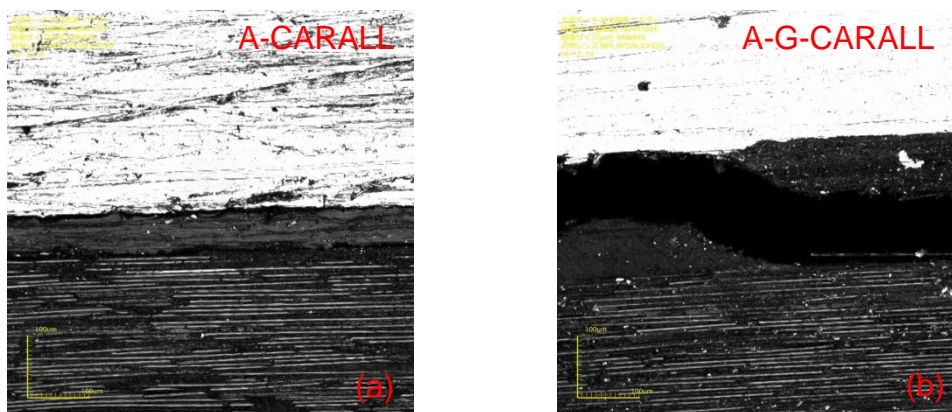

Figure 9. Crack propagation of A-CARALL and A-G-CARALL speimens

Figure 10 shows the fracture surface of three kinds of specimens which also confirm the aforementioned explanation. It can be found from Fig. 10(b) that there is more residual epoxy resin

on the fracture surface of A-CARALL specimen compared to CARALL specimen which indicates the more cohesive failure occurred in the A-CARALL specimen. Therefore, the fracture toughness of A-CARALL is higher than that of CARALL. From Fig. 10(c) we can see there are some fractured carbon fibers in the groove position which play a "bridging" role to resist the delamination propagation. Moreover, there is more cohesive failure than the A-CARALL specimen due to the existence of patterned grooves. This may explain the higher G_{IC} of A-G-CARALL than that of A-CARALL.
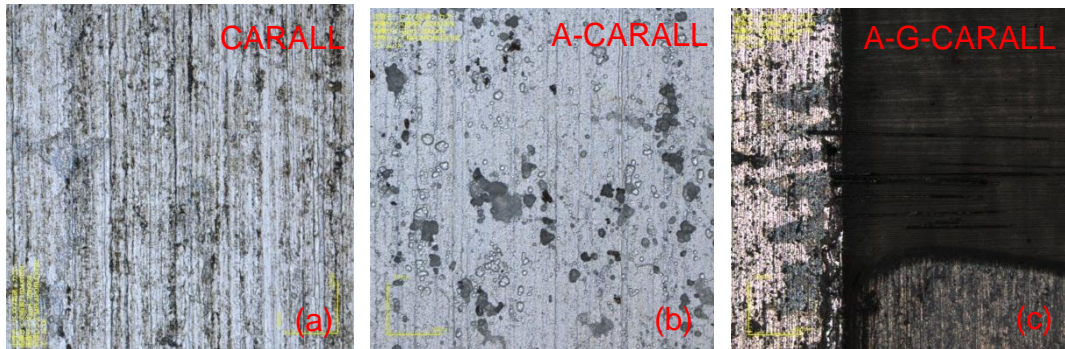

Figure 10. Fracture surface of (a) CARALL, (b) A-CARALL, (c) A-G-CARALL

For the second case, VGCF were included in the specimens. It can be found from Fig. 11(a) that almost all of the fracture surface were covered with residual epoxy resin and fractured fiber due to the proper addition of VGCF. This indicates that a lot of cohesive failure and "bridging" effect occurred on the fracture interface of A-CARALL(10) specimen. Therefore the fracture toughness was increased significantly compared with that of no VGCF. This is the same for Fig. 11(b), compared to A-G-CARALL, the residual epoxy resin and fractured fibers were left not only on the groove position but also on the flat part. This indicates that the flat part on the fracture surface of A-G-CARALL(10) was also contribute to the improvement of fracture toughness, which explains the enhancement of G_{IC} compared to A-G-CARALL specimens.
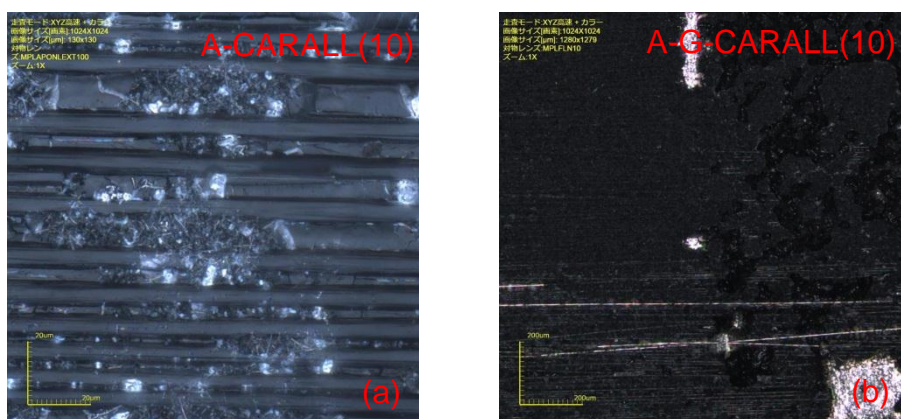

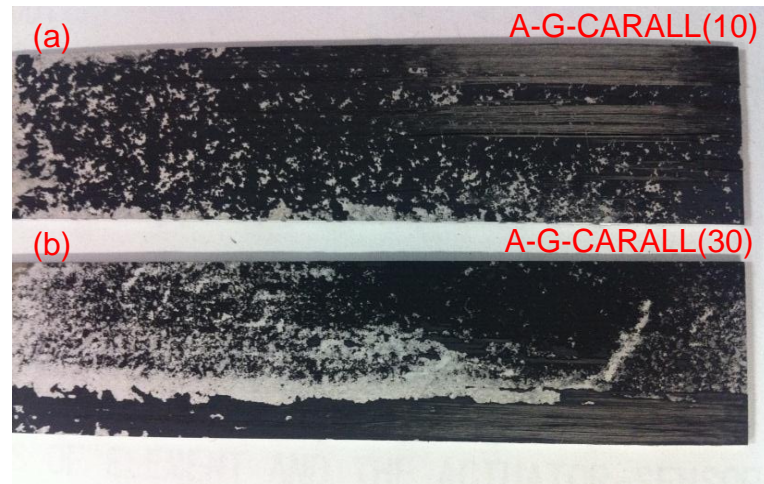Figure 11. Fracture surface of (a) A-CARALL(10), (b) A-G-CARALL(10)

Figure 12. VGCF dispersion condition of (a) A-G-CARALL(10), (b) A-G-CARALL(30)

From the above analysis, it reveals that the incorporation of proper content of VGCF at interface of the hybrid CARALL results in the enhancement of interlaminar fracture toughness. However, the overdose of VGCF in the interface of CFRP and aluminum alloy layer may cause the decrease of its fracture toughness. This may be explained by Fig. 12, which shows that the dispersion of VGCF on the A-G-CARALL(10) specimen is better than that of the A-G-CARALL(30) specimen. The VGCF agglomerate condition of A-G-CARALL(10) specimens was not so severe. However, when the VGCF area density reaches to 30 g/m^2, as shown in Fig. 12(b), the fracture surface containing some large defects caused by insufficient dispersion of VGCF can be seen clearly, which implies its lower fracture toughness.

4. Conclusions

In this study, we systematically investigated the effects of various toughing methods on the mode-I fracture toughness of hybrid CARALL. The following conclusions can be made:

1. When there is no VGCF addition, by carrying out DCB tests, the critical load and Mode-I fracture toughness of hybrid CARALL have been verified to be improved with acid etching treatment. And the patterned surface manufacturing on the aluminum alloy layers can further enhance the fracture toughness and resistance based on the acid etching treatment.

2. The fracture toughness of A-CARALL and A-W-CARALL was improved significantly by adding controlled amount of VGCF into the interface of CFRP and aluminum layer. However, the improvement was less for A-W-CARALL compared to that of A-CARALL. This indicates that, when VGCF was dispersed into the hybrid CARALL, the patterned surface may have a negative effect.

3. The reinforcement and toughening effects of VGCF interlayer depend on the area density of VGCF, which do not certainly increase as the addition amount of VGCF increases. The fracture toughness of the specimen first increases with the addition of VGCF, passes through a peak value, and then decreases. From the previous results, at least for the fabrication method described in this work, the best value of VGCF area density at the interface is 20 g/m^2.

References

[1] P.Y. Chang, P.C. Yeh, J.M. Yang, Fatigue crack initiation in hybrid boron/glass/aluminum fiber metal laminates. Materials Science and Engineering: A, 496 (2008) 273-280.

[2] Q. Yao, Modeling and characterization of interfacial adhesion and fracture. PhD thesis, Georgia Institute of Technology, USA, (2000).

[3] I.H. Yun, W.S. Kim, K.H. Kim, J.M. Jung, J.J. Lee, H.T.Jung, Highly enhanced interfacial adhesion properties of steel-polymer composites by dot-shaped surface patterning. Journal of Applied Physicals, 109 (2011) 074302.

[4] W.S. Kim, I.H. Yun, J.J. Lee, H.T. Jung, Evaluation of mechanical interlock effect on adhesion strength of polymer-metal interfaces using micro-patterned surface topography. International Journal of Adhesion & Adhesives, 30 (2010) 408-417.

[5] Q. Yao, J. Qu, Interfacial versus cohesive failure on polymer-metal interfaces in electronic packaging-effects of interface roughness. Journal of Electronic Packaging, 124 (2002) 127-134.

[6] C.J. Jang, W.S. Kim, H.C. Kim, J.J. Lee, J.W. Jeong, Study on the nano and micro surface morphology effects on interfacial strength of adhesively bonded biomaterials. Procedia Engineering, 10 (2011) 2585-2590.

[7] Jr. E.D. Reedy, N.R. Moody, J.A. Zimmerman, X. Zhou, M.S. Kennedy, W.M. Mook, D.F. Bahr, Effect of nanoscale patterned interfacial roughness on interfacial toughness. Sandia National Laboratories Report, USA, (2007).

[8] R.M.H. Jen, Y.C. Tseng, C.H. Wu, Manufacturing and mechanical response of nanocomposite laminates. Composites Science and Technology, 65 (2005) 775-779.

[9] M. Arai, Y. Noro, K. Sugimoto, M. Endo, Mode I and mode II interlaminar fracture toughness of CFRP laminates toughened by carbon nanofiber interlayer. Composites Science and Technology, 68 (2008) 516-525.

[10] Y. Li, N. Hori, M. Arai, N. Hu, Y.L. Liu, H. Fukunaga, Improvement of interlaminar mechanical properties of CFRP laminates using VGCF. Composites: Part A, 40 (2009) 2004-2012.

[11] JIS K 7086-1993. Testing methods for interlaminar fracture toughness of carbon fiber reinforced plastics. Tokyo: Japan Standards Association, (1993).